Pure & Appl. Chem., Vol. 58, No. 3, pp. 455–468, 1986.
Printed in Great Britain.

INTERNATIONAL UNION OF PURE AND APPLIED CHEMISTRY

MACROMOLECULAR DIVISION

COMMISSION ON POLYMER CHARACTERIZATION AND PROPERTIES

WORKING PARTY ON STRUCTURE AND PROPERTIES OF COMMERCIAL POLYMERS*

CHARACTERIZATION OF COMMERCIALLY AVAILABLE PAN (POLYACRYLONITRILE)-BASED CARBON FIBERS

Prepared for publication by

K. MORITA[1], Y. MURATA[2], A. ISHITANI[2]
K. MURAYAMA[2], T. ONO[1] and A. NAKAJIMA[3]

[1]Toray Ind. Inc., 2-2 Muromachi, Tokyo 103, Japan
[2]Toray Research Center, Inc., 1-1 Sonoyama, Otsu 520, Japan
[3]Kyoto University, Kyoto 606, Japan

for the Sub-Group meeting in Japan

Chairman: A. Nakajima; *Secretary*: T. Masuda;
Members: S. Hayakawa; M. Kato; Y. Kubouchi; T. Ono;
J. Shimizu; M. Uchida; A. Yoshioka

*Membership of the Working Party during 1983–85 was as follows:

Chairman: H. H. Meyer (FRG); *Secretary*: D. R. Moore (UK); *Members*: G. Ajroldi (Italy); R. C. Armstrong (USA); C. B. Bucknall (UK); J. M. Cann (UK); D. Constantin (France); H. Coster (Netherlands); Van Dijk (Netherlands); M. Fleissner (FRG); H.-G. Fritz (FRG); P. H. Geil (USA); A. Ghijsels (Netherlands); D. J. Groves (UK); H. Janeschitz-Kriegl (Austria); P. B. Keating (Belgium); H. M. Laun (FRG); C. Macosko (USA); J. Meissner (Switzerland); Millaud (France); A. Plochocki (USA); W. Retting (FRG); U. P. Richter (FRG); G. Schorsch (France); G. Schoukens (Belgium); J. C. Seferis (USA); J. M. Starita (USA); G. Vassilatos (USA); J. L. White (USA); H. H. Winter (USA); J. Young (Netherlands); H. G. Zachmann (FRG).

Characterization of commercially available PAN (polyacrylonitrile)-based carbon fibers

ABSTRACT: The characterization of high performance PAN-based carbon fibers is described. The process of conversion of polyacrylonitrile fibers into carbon fibers consists mainly of two sequent steps, namely stabilization and carbonization. The ladder structure consisting of acridone ring (40%), naphthyridine ring (30%) and hydronaphthyridine ring (20%) as shown in Fig.5 was assigned for the chemical structure of fully stabilized fibers. Structure characterization of carbon fibers was carried out by the use of the techniques such as scanning electron microscopy, transmission electron microscopy, electron diffraction and electron energy loss spectroscopy. Surface of carbon fibers and also the interface between the surface and the matrix plastics were studied utilizing various kinds of surface and microanalytical techniques. XPS has proven to be effective in obtaining useful informations. The use of additional techniques such as Raman microprobe, FT-IR, solid state high-resolution NMR and secondary ion mass spectrometry are described. The characteristic features of carbon fibers are high tensile modulus and high tensile strength combined with low specific gravity. Following items about mechanical properties of carbon fibers are discussed: multifilament tensile test which is useful for measuring tensile strength distribution of single filaments, relation between tensile strength of filaments and structural parameters, and relation between tensile strength of filaments in air and those within composites.

1 INTRODUCTION

High strength, high modulus carbon fibers are finding increased use in composite applications. Polyacrylonitrile (PAN) is now regarded as the most preferable precursor material for these fibers. Shindo of Osaka Industrial Institute of Japan succeeded in making carbon fibers from PAN in 1959 firstly in the world, and reported the detail in 1961(1). Nippon Carbon and Tokai Electrode (now Tokai Carbon) were the pioneers in the development of PAN-based carbon fibers. Nippon Carbon started commercial production of PAN-based fibers at the scale of a half metric ton per month in 1962.

In 1963(2), scientists of Royal Aircraft Establishment in England had found that the tensile strength of carbon fibers can be improved by restraining the fibers from shrinking in the first thermal treatment step. Companies in England started production of PAN-based carbon fibers in 1964. Thereafter, Toray and Toho Beslon, the producers of PAN fibers in Japan, started commercialization of PAN-based carbon fibers in 1971 (ten metric tons per year) and 1973 (five metric tons per year), respectively. Since then, a very high degree of interest in the use of carbon fibers for reinforcement of plastics sprang up. The demand for high performance carbon fibers was approximately ten metric tons in 1971 but it increased to two thousand metric tons in 1984. Sixteen companies in the world are now producing PAN-based carbon fibers. Steady improvements have been made in the mechanical properties of carbon fibers since their commercial introduction. The purpose of this article is to review the present status of characterization of commercially available PAN-based carbon fibers. The characterization of the stabilized fibers, the intermediate products of the process, will also be discussed because they are also commercially important.

2 CHEMICAL STRUCTURES OF THE STABILIZED FIBERS

The chemistry of conversion of PAN into carbon fibers consists of two sequent steps: stabilization of PAN (I) into the condensed heterocyclic ring stucture (II) prior to further treatment, and a high-temperature condensation of the intermediate into the two dimensional graphite-like structure (III) (Fig.1).

Although copolymerization of PAN with comonomers bearing oxygen moieties such as carboxylic and hydroxyl can initiate nitrile polymerization, full polymerization of nitrile can not be attained in this way by two reasons: (a) atactic stereochemical

conformation of the polymer chain inhibits the access of two nitrile groups after polymerization of a limited number of nitrile groups and consequently terminates the polymerization, and (b) only small percentage of uniform copolymerizaton can take place by the present technology(3a).

Further stabilization is therefore necessary and it is generally achieved by air-oxidation. The oxygen containing moieties derived by the oxidation of the condensation intermediates can initiate further polymerization of nitrile groups. Similar initiation has been known to be carried out by the sulfur containing moieties derived by the reaction with sulfur(3b).

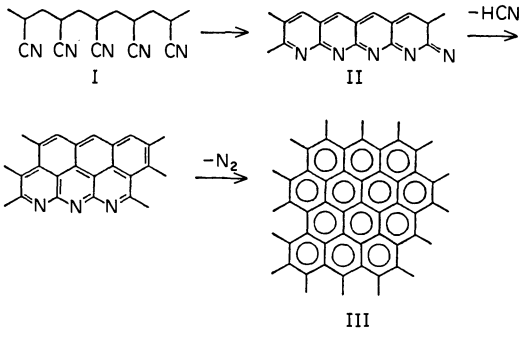

Fig. 1 Chemistry of conversion of PAN into cabon fibers

Conventional spectroscopic techniques such as the solution nuclear magnetic resonance spectroscopy (NMR) and the dispersion type infared spectroscopy (IR) have failed to give sufficient data to determine the chemical structure of the stabilized PAN fiber, because stabilized PAN fibers are insoluble in any kinds of organic solvents and it has also intense absorption due to electronic transition over the whole infra-red region. Nevertheless, various kinds of the chemical structure models have been proposed for stabilized PAN on the basis of evolving gas analysis and data from spectroscopic techniques(4). But these are not decisive enough to fully understand the chemical structure of the stabilized fibers.

Combination of the recently developed techniques in solids such as high resolution NMR techniques in solids, i.e., cross polarization/magic angle spinning techniques and X-ray photoelectron spectroscopy (XPS) enabled us to fully confirm the structure.

By oxidation of PAN fibers at 240°C for 5.2 hours, new peaks appear in the low field region of C-13 NMR spectrum indicating formation of unsaturated carbons as shown in Fig 2C. By heat treatment of PAN with sulfur at 220°C for 2 hours and subsequently at 300°C for 10 hours, similar spectrum (Fig.2B) except the lowest magnetic field peak (177ppm) was obtained. The similarity of two spectra indicates that the structure of sulfur treated PAN is analogous to that of air treated PAN except the absence of oxidised carbon atoms. Assignment of the spectra is based on chemical-shift comparison with model compounds (Fig.3)(5). Confirmation of the assignment is obtained from the nonprotonated C-13 NMR spectrum (Fig.2D) measured by using the technique described by Opella and Fray. Signals from protonated carbons are suppressed because of much greater C-13 and H-1 dipolar

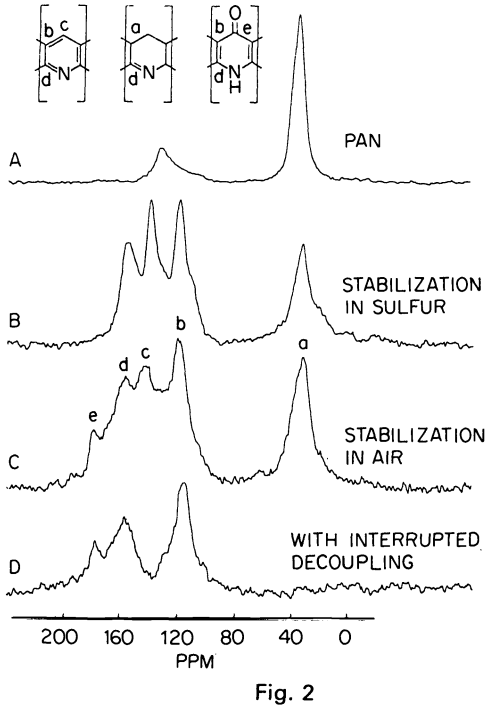

Fig. 2

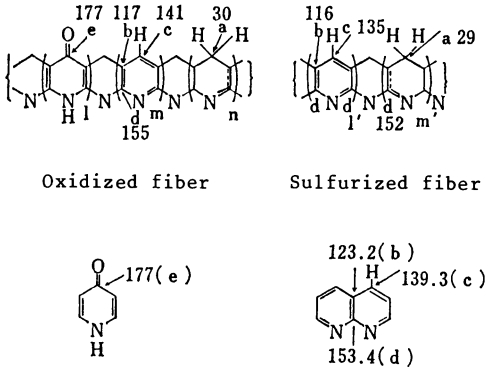

Fig. 3

Fig. 2 Carbon-13 CP/MAS NMR spectra of (A) PAN (B) heat treated PAN in sulfur at 220 C°for 2hr and then at 300°C for 10hr, (C) heat treated PAN in air at 240°C for 5.2hr, and (D) nonprotonated C-13 spectrum of sample (C)

Fig. 3 Assignment of NMR of stabilized fibers (Cf. Fig. 2)

interaction than for nonprotonated carbons. Therefore, signal a and c are assigned to protonated carbons and signal b, d and e to nonprotonated carbons clearly.

X-ray photoelectron spectra of O1s and N1s in the stabilized PAN oxidized at 240°C for 310 min are curve-resolved and assigned as shown in Fig.4 (6). The O1s spectrum consists of two components, the lower bonding energy component with 80% intensity is assigned to acrydone type carbonyl and the other one with 20% intensity is assigned to normal carbonyl and alcohol group. The N1s spectrum has two components which are assigned to nitrogen in acrydone ring (40%) and the one in naphthyridine and hydronaphthyridine rings (60%). XPS spectrum of C1s in the oxidized PAN heated at 240°C for 310min are also curve resolved and shown in Fig.5. A signal b with 40% intensity is assigned to carbon atoms adjacent to nitrogen atoms, signal a with 45% intensity to other carbons and signal c with 15% intensity to carbonyl carbons. The ladder structure shown in Fig.6 was estimated as the chemical structure for fully stabilized PAN(6).

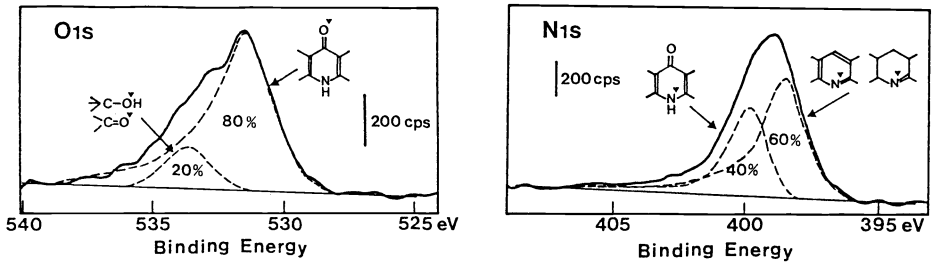

Fig. 4 XPS O1s and N1s spectra of thermally stabilized PAN

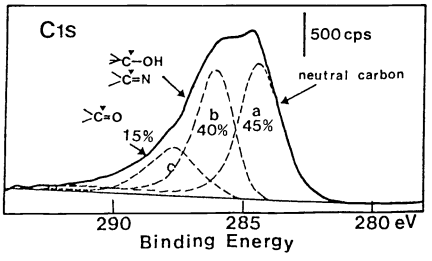

Fig. 5 XPS C1s spectrum of thermally stabilized PAN

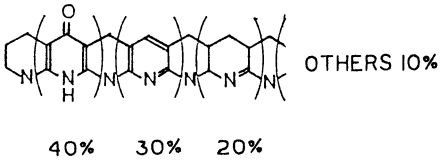

Fig. 6 Chemical structure of fully stabilized fiber

3 STRUCTURE CHARACTERIZATION OF CARBON FIBERS

Scanning Electron Microscope (SEM) SEM has been widely applied to observe the texture of sides and fracture ends of carbon fibers as well as composites. Carbon fibers are electronically conductive, so that surface coating with the conductive material is unnecessary in general purpose. But small amount coating with metal can emphasize the surface roughness down to 50Å. Recently SEM equipped with a field emission gun, that is, FE-SEM became available in the industrial laboratory. Resolution power of SEM has been increased up to 20-30Å at low accelerating voltage (for instance, 1kV voltage). Low voltage operation is of a great advantage in the sense to avoid specimen damage.

Fig.7 shows a FE-SEM micrograph of fracture ends of high modulus (HM) carbon fiber. A detailed structure was clearly resolved at the fracture ends and the side of fiber. Observation was carried out with small amount of coating at low voltage (5kV). The result is helpful to the study of fracture mechanism. A close observation also reveals an internal texture as well as skin structure.

Transmission Electron Microscope (TEM) SEM provides morphological information about overall of carbon fibers, but little information about internal structure. While transmission electron microscope (TEM) gives fruitful information about the internal structure of materials. Magnification is in the range of 10^3x to 10^6x. And resolution power is now in the order of 1-3Å. The direct structure image of graphite layer grown within carbon fiber can be obtained on a fluorescence screen at high magnification. High resolution structure image enables us to study the crystallinity, orientation and texture difference between inside and outside in carbon fiber. It is well established in the light of electron optics that there is one-to-one correspondence between real structure

Fig. 7 FE-SEM of HM carbon fiber

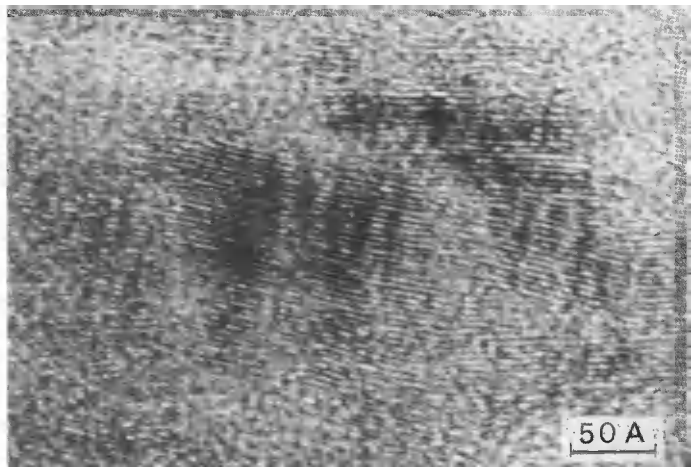

Fig. 8 Longitudinal section of HM carbon

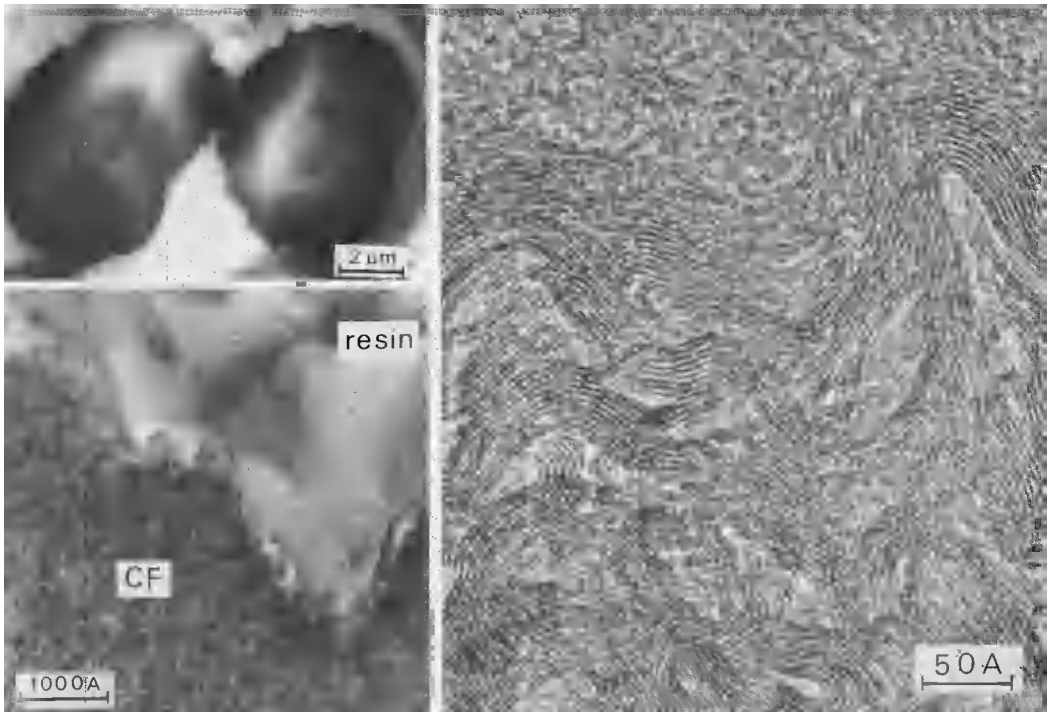

Fig. 9 Transverse section of HM fiber

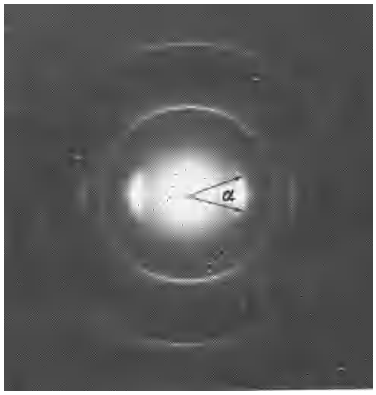

Fig. 10 Electron diffraction pattern of HM carbon fibers

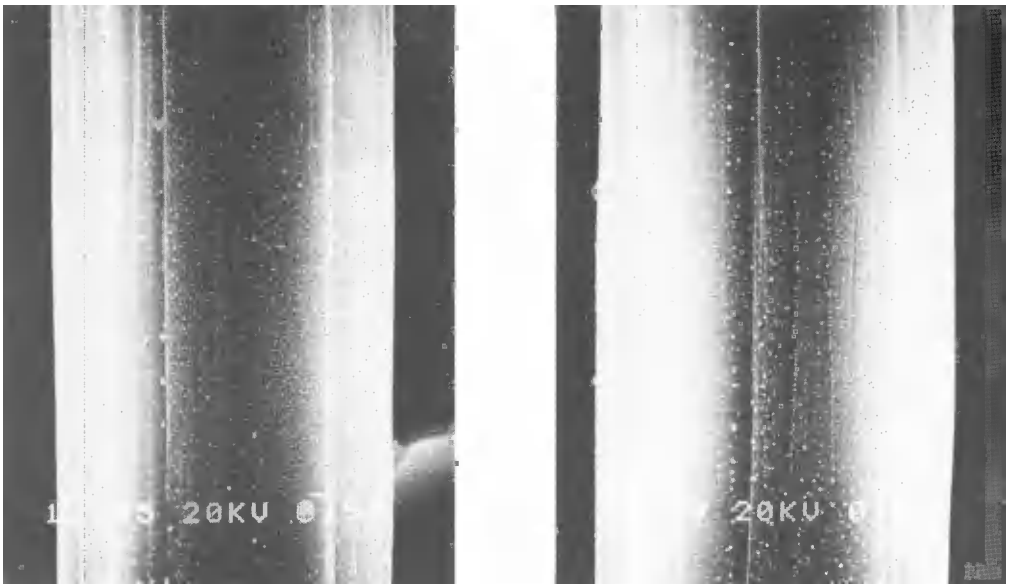

x 10000

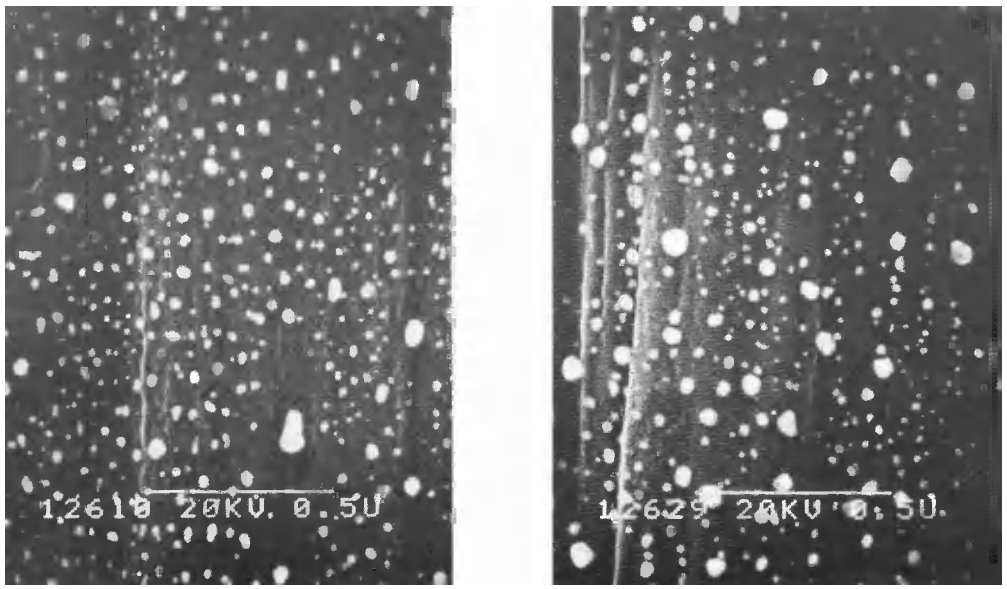

x 80000

1000 Å

Graphite Fiber

Carbon Fiber

Fig. 21 Field emission scanning electron micrographs of Ag island film (60Å) on carbon fibers

and high resolution image under the optimum condition. For microscopic observation, however, thin section of carbon fiber has to be prepared by suitable process. Specimen preparation of this section may require a high skill.

Fig.8 shows a high resolution micrograph of a longitudinal thin section of PAN based HM fiber near the fiber surface. Crystallinity of graphite can be estimated from the figure. Another example is one of transverse section of carbon fiber as shown in Fig.9. Transverse sectionning in the manner of small damage is very difficult technique. The transverse section was prepared by ion milling after embedding into a proper resin. The high resolution micrograph shows directly a fine structure of a boundary and also orientation of small graphite crystallites. Combination of transverse and longitudinal observation can permit a determination of three dimensional construction of carbon fibers.

Electron Diffraction (ED) TEM has a function of a selected area electron diffraction (SAED) mode as well as normal imaging mode, therefore a quantitative information of crystallinity, crystallite size (Lc, La) and orientation of crystallites in the submicron range can be obtained.
Spatial resolution usually recommended is in the order of 0.5-1.0 μm diameter. However, improvement of spherical aberration of the objective lens enable us to minimize the area selection down to 0.5 μm. Furthermore in STEM (Scanning Transmission Electron Microscope) mode, electron probe well collimated narrower than 200Å can be irradiated onto the interested area and then μ-ED pattern can be formed. Fig.10 shows an electron diffraction pattern of HM carbon fibers. Angle $\alpha/2$ as indicated in the figure defines the orientation of graphite crystallites along fiber axis. The Lc value depends on full width of half maximum (FWHM) of (002) diffraction spot.

Electron Energy Loss Spectroscopy (EELS) When electron beam with incident energy E passes through the thin specimen, a part of energy is adsorped into the specimen, depending on both compositional element and bonding state. As well known elemental analysis can be made by EELS, especially sensitive to light element. At the characteristic adsorption edge, fine structure is often observed. The fine structure depends on chemical state. Many researchers studied extensively the electron energy loss. For example, energy loss spectrum of graphite and amorphous carbon film are shown in Fig.11. Apparent difference between both is obvious at the fine structure. Amorphous carbon has a simple peak in the vicinity of 285 eV, while in the graphite, fine peaks appear which may be assigned to interband transitions, that is, $\pi \rightarrow \pi^*$ and $\sigma \rightarrow \sigma^*$, respectively.

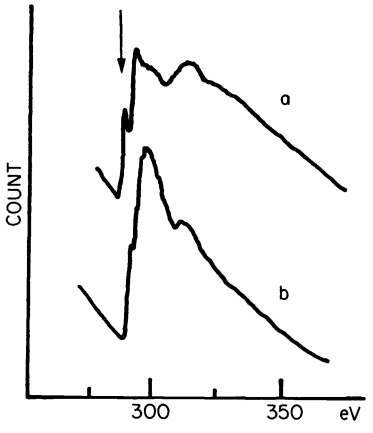

a: loss spectrum of graphite,
b: loss spectrum of amorphous carbon

Fig. 11 Electron energy loss spectra

So the appearance of fine details is applicable to qualitative estimation of crystallinity of graphite in carbon fiber and also difference of crystallinity between inside and outside of fiber.

The characterization of carbon fiber by using electron optics. The direct imaging of graphite crystal can help the 3-dimensional construction of carbon fiber model, especially about crystal size and orientation near fiber surface. Electron diffraction provides the average information of crystallinity and prefered orientation in submicron area. Combination of high resolution image with ED results permits refinement of carbon fiber model as described above. Furthermore EELS gives us the data on bonding state.

4 SURFACE AND INTERFACE ANALYSIS OF CARBON FIBERS

Surface Composition and In Depth Profiles of Carbon Fibers XPS has started to be used to characterize surface compositin of carbon fibers frequently(7,8,9,10). Argon ion etching can be used to reveal heterogeneous structures of the carbon fibers in the depth direction. Figs.12 and 13 show the results on the high tensile strength (HT) carbon fiber and the high modulus (HM) fiber. Here, HT is obtained by heat treatment up to about 1500°C, whereas HM is prepared by treatment over 2000°C. Both of HT and HM have substantial amount of oxygen which is analyzed to originate from alcoholic and also carbonyl groups before any surface oxidation is conducted. They are considered to be introduced onto the surface by quenching of the free radicals which are produced in the inert gas atmosphere

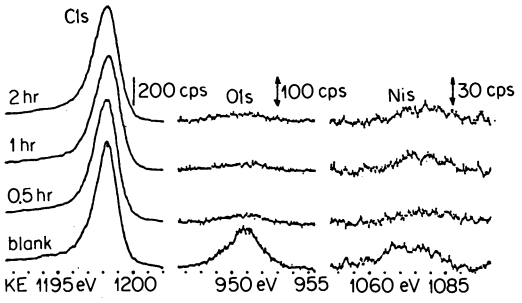

Fig. 12 The etching effect on HT

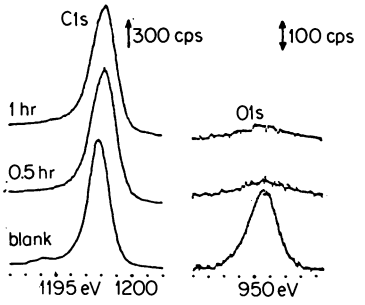

Fig. 13 The etching effect on HM

of the furnace at high temperature, when the fibers are brought into air. The oxidized layers thus created in both of HT and HM are thin and removed quickly with the 0.5hr etching. The N1s peak due to the residual nitrogen of HT does not show much intensity variation, although the center of the peak shifts about 2eV to lower B.E. values by the etching, indicating the presense of more oxidized nitrogen species on the surface than bulk composition.

Line Shape Analysis of C1s Peak of XPS for Evaluation of Surface Graphitization Degree(12)

Line Shape analysis of asymmetric C1s peak of XPS due to excitation of the extended electron conjugation of graphite planes(11) can be used for evaluation of surface structure of carbon fibers. Fig.14 shows C1s line shapes of various kinds of carbon materials with different graphitization degrees. FWHM values decrease systematically with increased graphitization degree. Four kinds of carbon fibers prepared at different temperatures are examined as well by XPS together with Raman spectrum and Xray diffraction as indicated in Fig.15. Three kinds of parameters obtained from three techniques are plotted against the baking temperature in Fig.16, where XRD gives bulk, Raman gives mid-surface down to several hundred A depth, whereas XPS gives the outermost surface information of graphitization degree.

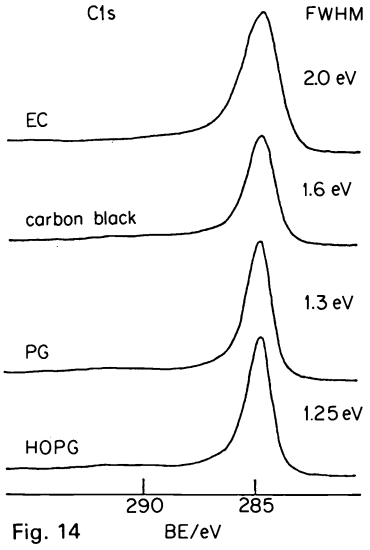

Fig. 14

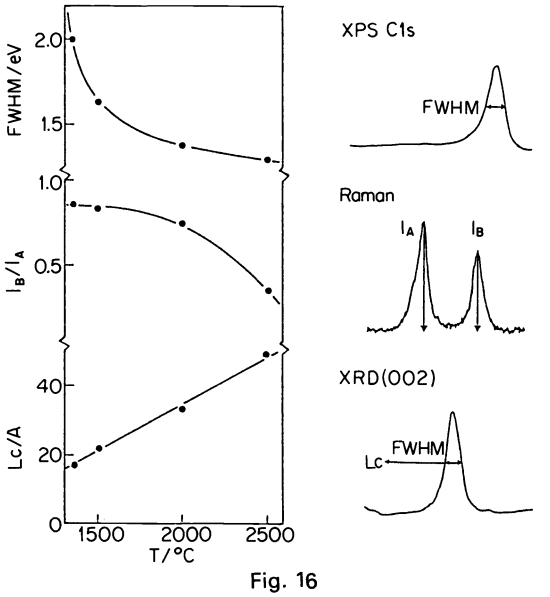

Fig. 16

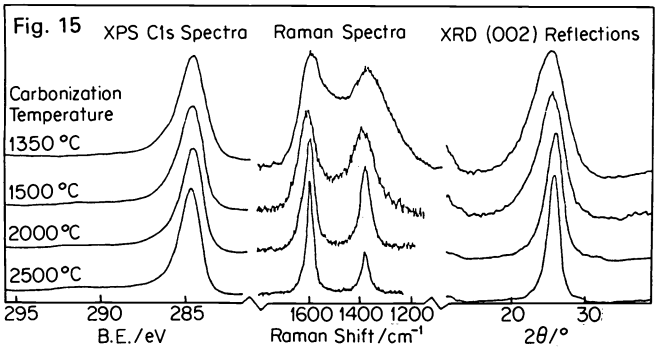

Fig. 14 Line shapes of C1s peaks of various kinds of carbon materials

EC: Evaporated carbon
PG: Pyrolytic graphite
HOPG: Highly oriented Pyrolytic graphite

Fig. 15 Comparison between three kinds of techniques on carbon fibers prepared at different temperature

Fig. 16 Parameters of graphitization degree obtained from three kinds of techniques

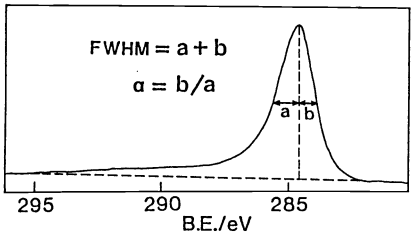

Fig. 17 Parameters of the line shape analysis defined from a typical XPS C1s spectrum

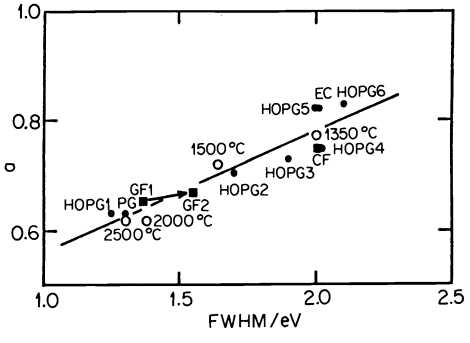

Fig. 18 Correlation found between the asymmetric parameters and FWHM of C1s peaks of various carbon samples
HOPG1,2,3,4,5,6: Control; highly oriented pyrolytic graphite (HOPG) and Ar^+ ion bombarded HOPG for 2s,10s,30s,1min and 5min
PG: Pyrolytic graphite
EC: Evapolated carbon
GF1,2: HM and surface treated HM
CF: HT
Open circles: Carbon fibers prepared at various temperature

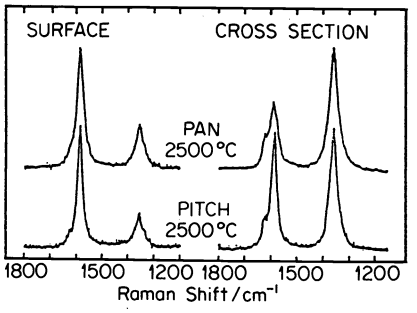

Fig.19 Raman spectra of the surface and the cross section of HM carbon fiber

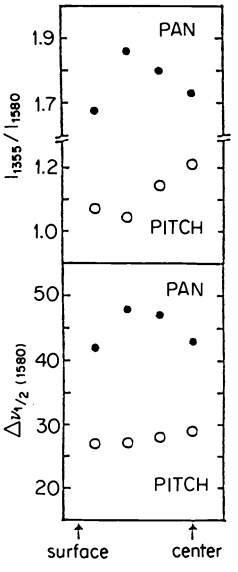

Fig.20 Correlation found between asymmetric parameters and FWHM of C1 peaks of varions carbon samples

An asymmetric parameter of C1s line is tentatively defined as in Fig.17. This parameter has very good correlation with FWHM as indicated in Fig.18. It may be explained by difference of life time of C1s electron hole determined mainly by Auger process between well and poorly organized graphite structures. Both parameters of FWHM and the asymmetry factor can be used well for surface evaluation of carbon fibers.

Raman Microprobe Analysis of Surface and Bulk Structures of Carbon Fibers Evaluation of lattice structure of carbon materials is frequently done by Raman Spectroscopy(13,14,15). Most of carbon materials of graphite-like structure with valence electrons in sp^2 hybrid orbitals have intense Raman bands at 1580cm^{-1} and 1360cm^{-1}. A perfect single crystal of graphite has a sharp single band at 1580cm^{-1}. Any kind of inperfection brought into the single crystal is sensitively detected by spectral changes in this wavenumber region as follows, (a) an additional band appears at 1360cm^{-1}, (b) the band at 1580cm^{-1} shifts to higher wavenumber and a new spectral component appears at 1620cm^{-1} as a shoulder of the band, (c) widths of both of the bands increase.

Both surface and small area analysis of carbon materials become possible with Raman techniques. Use of visible and ultraviolet radiation for excitation enables focusing the probing beam easily down to 1 m by an optical microscope(16,17). Intense light absorption of carbon materials limits penetration of the incident beam to a few hundred Å, thus making the technique surface sensitive. Further improvement of surface sensitivity can be achieved by utilization of the Surface Enhanced Raman Scattering (SERS) effect to detect a monoatomic layer on surface exclusively(18).

Cross sections of two kinds of HM fibers made from PAN and coal pitch by baking at 2500°C were prepared. Their Raman spectra are compared with the commonly measured fiber surface which corresponds to basal plane of graphite. Preparation of finely and equally polished cross sections is essential in the experiment to avoid any artifacts comming from difference of roughness of the cross sections. Fig.19 indicates comparison of surfaces and cross sections of PAN and pitch fibers. Raman spectra of both fibers in cross sections show spectral features indicating more irregular graphite lattice structure than in surface. The pitch fiber is also revealed to have more advanced stage of graphitization than PAN fiber either on surface or on cross section.

Heterogenity of graphite fibers in the radial direction can be studied by Raman microprobe by scanning the focused beam on the cross sections of the fibers. Fig.20 indicates preliminary results of such experiment. Two parameters, intensity ratio between the bands at 1355 and 1580cm^{-1}, and FWHM are plotted in depth direction from the surface to the center of the fiber. The result indicates that the PAN based HM fiber has higher graphitization areas both in the surface and in the center of the fiber, while, the pitch fiber is more graphitized in the surface.

The modulus of PAN based HT(28) and HM(19a) fibers across the fiber diameter were measured by successively oxidative milling away the fiber surface. The milling was possible only down to about one third of the radius because of experimental difficulties. The decrease in fiber modulus as the surface is etched away was observed. The results agree with the observation of the above mentioned Raman microprobe experiment. It should be noted, however, that the observation of higher graphatization area in the center of the HM fiber is contrary to the previous assumption (19b).

Further enhancement of surface sensitivity of Raman scattering can be attained by the Ag overlayer technique(18). Thin Ag island films of average thickness of several scores A are evaporated on carbon fibers surface. Raman scattering from the outermost surface is exclusively enhanced by the Ag films possibly due to the electromagnetic mechanism based on the excitation of surface plasmon.

The FE-SEM images shown in Fig.21 indicates small Ag islands necessary to raise the SERS effect. Fig.22 shows the Raman spectra of graphite fibers covered with the Ag films of 51 and 106Å thickness, where enhancement of the spectrum is clearly observed. The band at 1350cm^{-1} due to the disordered graphite structure is more enhanced than one at 1580cm^{-1},

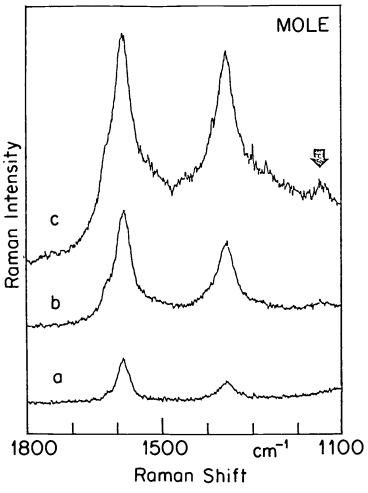

Fig. 22 Raman spectra of HM covered by Ag island films.
(a) control, (b) 51Å, (c) 106Å

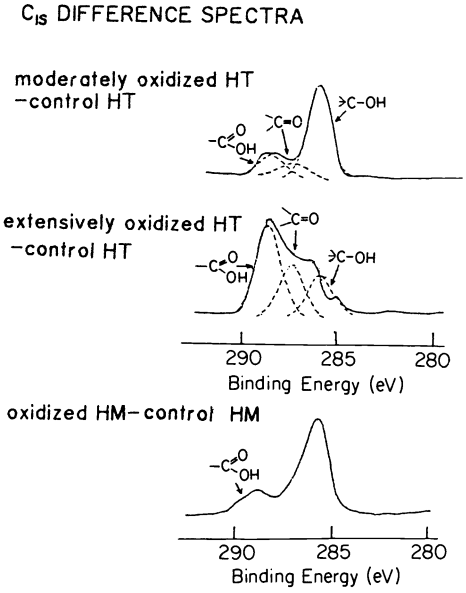

Fig. 23 Digital differnce spectra of surface freated HT and HM

indicating the existence of more disordered structure in the vicinity of the outermost surface. A newly detected band at 1140cm^{-1} in the enhanced spectrum may be due to c-c stretching vibration of polyene-like structure existing only at the surface.

Functional Groups Generated by Surface Oxidation The digital difference spectrum technique on XPS is used for the qualitative analysis of surface functional groups generated by the surface oxidation(21,22,23,24). The difference spectra were obtained by subtraction of C1s spectrum of control HT and HM from that of oxidized HT and HM respectively. The obtained C1s difference spectrum of HT has three components with chemical shifts corresponding to hydroxyl groups (C-OH;286eV), carbonyl groups (C=O;287eV) and also carboxyl groups (-C$^{O}_{OH}$,288.6eV) as indicated in Fig.23. The chemical composition of the surface of HT after the moderate oxidation is 73% of hydroxyl group, 17% of carboxyl group and 10% of carbonyl group. On the other hand, the composition produced by the extensive oxidation consists of 24% of hydroxyl group, 22% of carbonyl group and 54% of carboxyl group.

Figure 21 is printed on page facing p.459

The interlaminar shear strength (ILSS) of composites increased on the moderate oxidation of carbon fibers, but decreased on the subsequent excessive oxidation. It is conceivable that the excessive oxidation degrade the graphite layer at the surface and hence forms the weak boundary layer.

These functional groups generated by the surface oxidation disappear completely with thermal treatment at 1000°C in vacuo for 0.5 h, and the surface oxygen concentration returns to the level of the control when the fibers are brought into air by quenching the free radicals.

The difference spectrum of HM in Fig.23 has two components. The higher binding energy component at 288.7eV which disappears after thermal treatment at 1000°C is assigned to carboxyl group ($-C\overset{O}{\underset{OH}{<}}$), and the lower binding energy peak which is left after the thermal treatment is attributed to disordering of graphite crystal lattice brought about by the surface oxidation and/or to hydroxyl group.

Chemical Modification of Carbon Fiber Surface Coupled with XPS Measurement Functional groups brought on HT surface by surface oxidation can be studied more in detail and more quantitatively by XPS measurement accompanied with the chemical modification reaction(12). In situ measurement suffers from small sensitivity and lack of chemical shifts large enough to differentiate functional groups generated on surface. The purpose of the chemical modification is to convert a specific functional group to a chemical species which is easier to discriminate sensitively and to quantify by XPS.

Fig.24 indicates typical chemical modification reactions favorable to use on functional groups on HT surface(25). Combined use of these reactions can differentiate three kinds of functional groups and quantify them more sensitively by using the F1s signal of reagents. Comparison of control and an oxidized HT after two kinds of chemical modification reactions is illustrated in Fig.25. Increase of F1s signals by surface oxidations is clearly seen in the spectra.

Surface Composition and the Bonding Property to the Matrix Resin Estimation of the bonding strength between the carbon fibers and the matrix resin is extremely difficult because of the morphology of the fibers. Here the interlaminar shear strength (ILSS) of the composite prepared from the carbon fibers and epoxy resin is related to the O1s/C1s ratio of XPS which is well established(7) to represent the amount of the functional groups on the carbon fibers surface.

The surface oxidation increases the O1s/C1s ratio and ILSS simultaneously both for HT and HM as shown in Fig.26(26). A good linear relation is observed for HT. The thermal treatment in vacuo decreases the O1s/C1s ratio and ILSS reversibly in HT. Therefore, introduction of the functional groups on the surface is a main factor for the bonding property. On the other hand ILSS does not decreases in HM with the thermal treatment although the O1s/C1s decreases. It may indicate that physical perturbation such as roughness or irregularity of the lattice structure brought on the surface by the treatment determines the bonding property. The hydroxyl group formed by quenching the remaining radicals after decarboxylation may also play the role for the bonding properties. There is an explanation (27) that untreated HM fibers have the weak graphitic boundary layer which is removed with epoxy resin at break and hence exhibits low ILSS. Surface treatment removes the weak layer.

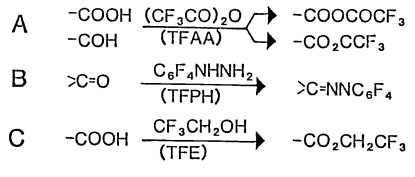

Fig. 24 Chemical modification reactions

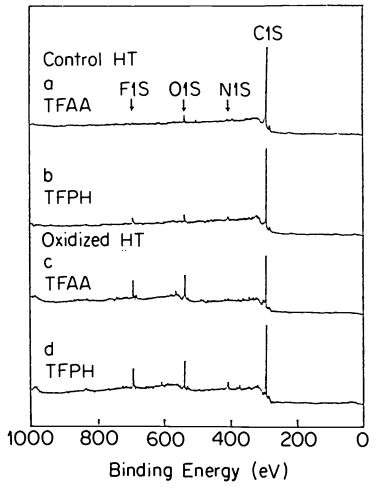

Fig. 25 XPS Spectra of HT after the chemical modification

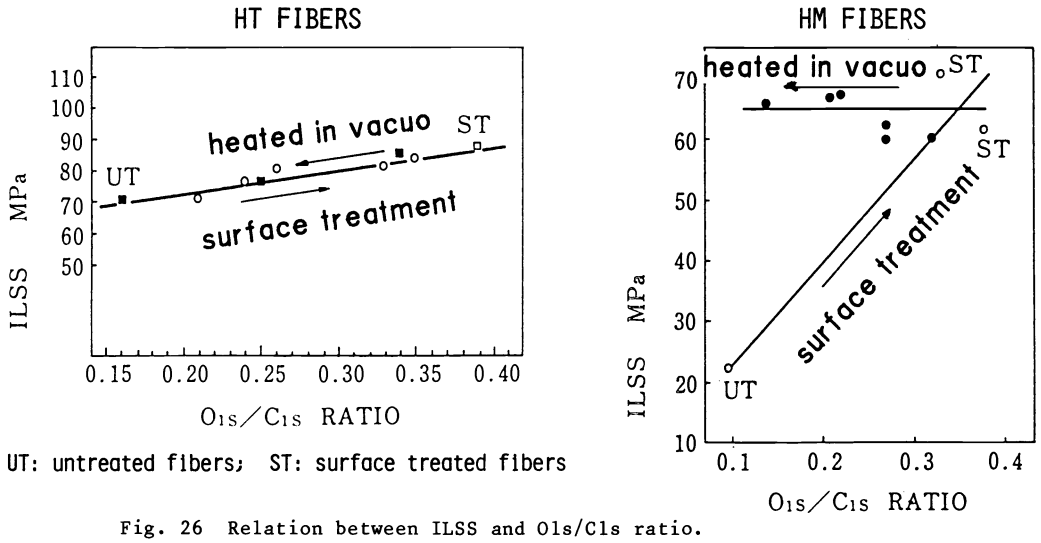

Fig. 26 Relation between ILSS and O1s/C1s ratio.

New techniques for surface and interface characterization of carbon fibers

FT-IR The high sensitivity and the extensive data processing capability of FT-IR contribute much to carbon fiber works. A FT-IR reflection-absorption spectrum of the surface oxidized HT is shown in Fig.27. A band at 1680cm^{-1} is identified and assigned to the carbonyl stretching vibration of the aromatic carboxyl group. A FT-IR-ATR digital difference spectrum also reveals thermal oxidation of an epoxy polymer thin film on an extensively surface oxidized HT.

AES and ELS Electron probe techniques like Auger Electron Spectroscopy (AES) and Electron Energy Loss Spectroscopy (ELS) will have interesting application on evaluation of carbon fiber surface. AES can give composition of relatively high concentration elements such as residual oxygen and nitrogen, and also surface contaminants. Possibility of focusing of electron beam down to 0.1 m is convenient to measure a single filament, for analysis of longitudinal distribution of either oxidation degree or contamination for an example.

High resolution AES spectra of carbon KVV transition give information of surface carbon structure. Fig.28 gives AES spectra of various carbon materials. Peaks A and B correspond to Auger processes due to σ electrons and change shapes with carbon struture, peak C represents a component by π electrons.

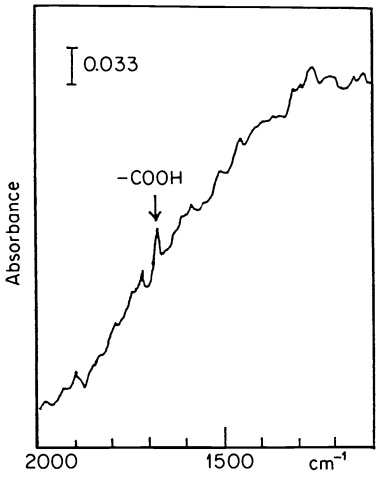

Fig. 27 A FT-IR-RAS spectrum of a surface oxidized HT carbon fibers

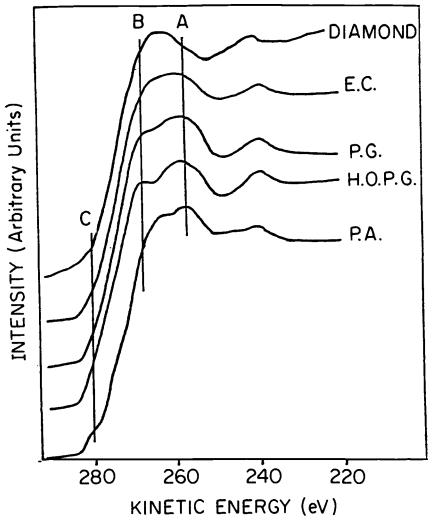

Fig. 28 Carbon KVV Auger spectra of various kinds of carbon materials.
E.C. : Evaporated carbon
P.G. : Pyrolytic graphite
H.O.P.G. : Highly oriented pyrolytic graphite
P.A. : Polyacetylene

ELS may give complementary information to AES. Fig.29 shows variation of the ELS spectrum of diamond by Ar^+ ion etching. Appearence of the π-electron peak and change of the plasmon peak shape suggest generation of amorphous carbon like evaporated carbon or glassy carbon on the surface by Ar^+ ion etching.

High Resolution Solid NMR The cross polarization/magic angle spinning(CP/MAS) and the other modes of the techniques are expected to observe the surface and the interface area selectively. The discussion on the interaction between the carbon fiber surface and the matrix resin will be possible because of the detailed structural information from NMR.

Secondary Ion Mass Spectrometry (SIMS) Detection and imaging of the low concentration elements on the carbon fiber surface as well as their depth profiles are available from this technique.

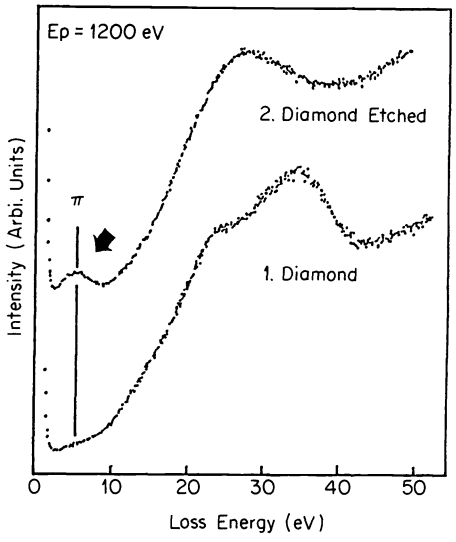

Fig. 29 ELS apectra of diamond and Ar^+ into etched diamond

5 MECHANICAL PROPERTIES OF CARBON FIBERS

Remarkable improvements have been made in the mechanical properties of HT carbon fibers recently. Progress of tensile strength of PAN-based carbon fibers in the case of TORAYCA (carbon fibers from TORAY) is shown in Fig.30. The values displayed in the straight line are for commercial products and those in the dotted line are experimental. High performance fibers with a breaking strain over 2% measured in composites were reported by TORAY in 1977 firstly in the world(28).

Multifilament Tensile Test Method Measurements of the mechanical properties of carbon fibers are usually carried out with the impregnated and cured strands, since the results obtained by this method correlate better with the composite properties of fibers than those obtained by the single-fiber method. However, measurements of tensile strength distribution of single filaments become important when theoretical consideration is carried out. McMahon proposed a tensile testing of carbon fiber bundle composed of several hundred filaments(29). Noguchi and one of the authors proposed a tensile test method in which about twenty to thirty single filaments are tested simultaneously(30). According to this method the load elongation curve appears as a kind of a broken line A1B1, A2B2, A3B3 etc. as shown in Fig.31 which correspond to breaking load of single filaments. Distribution of tensile strength of single filaments is thus obtained quickly.

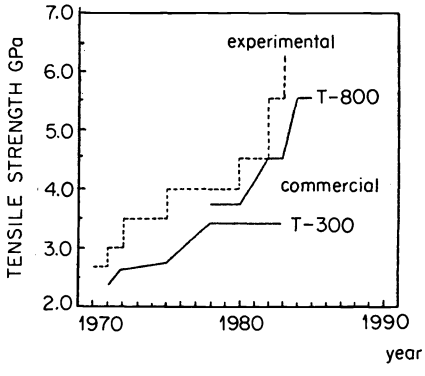

Fig. 30 Improvement of tensile strength of carbon fibers

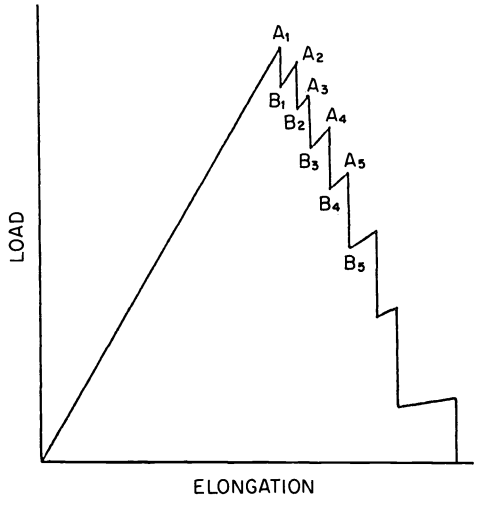

Fig. 31 A typical pattern of load-elongation curve of a bundle

In Fig.32, comparison between the conventional single filament method and the present method (multifilament method) is shown. As a whole, coincidence is fairly good, but some load difference between two methods is seen at the low tensile breaking load region. In the multifilament method, filaments are taken out from a yarn at a time, so that even weak filament can be measured, while in the conventional filament method each single filament is taken out one by one, so that the weak filaments are apt to break at the sampling process before tensile testing. As shown above, multifilament test method is relatively simple, efficient and it takes 1/10 times compared to single filament method. Moreover it is sensitive in detecting whole feature of tensile strength distribution. By using this method, it would become possible to investigate the relation between the strength distribution of single filaments in air and those within composites, and also the relation between the strength of single filament and structural parameter of the fiber.

Relation between Tensile Strength of Filaments in Air and that in Composites Carbon fibers are in almost all cases used as composite materials, so that tensile strength within composites is more important than that in air, and it is important to correlate both tensile strengths. There are several theoretical analyses in which distribution of tensile strength of fibers is taken into account; there are few reports which compared them with experimental results.

According to Rosen(31) tensile strength of filaments in a composite is given by the tensile strength of a bundle at a small gage length (eq.(1)).

$$\sigma_c = (l\alpha\beta e)^{-1/\beta} \qquad (1)$$

where α and β are Weibull parameters of the tensile strength distribution of single filaments. The shape of the distribution of tensile strength of single filament is given by eq.(2).

$$F(\sigma) = 1 - \exp(l\alpha\beta\sigma) \qquad (2)$$

where $F(\sigma)$ is a cumulative distribution function, σ is a tensile strength of a single filament, l is gage length. Ineffective length l was determined to fit to the experimental results. The correlation was best when l=0.6mm.

Fig.33 shows several examples of the shape of the tensile strength distribution. Weibull parameters were obtained by measuring tensile strengths distribution of

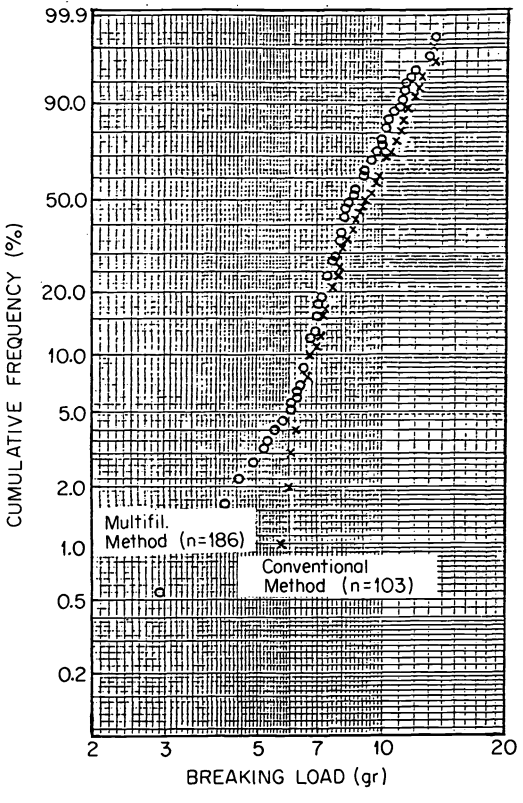

Fig. 32 Comparison between multifilament method & conventional single filament method

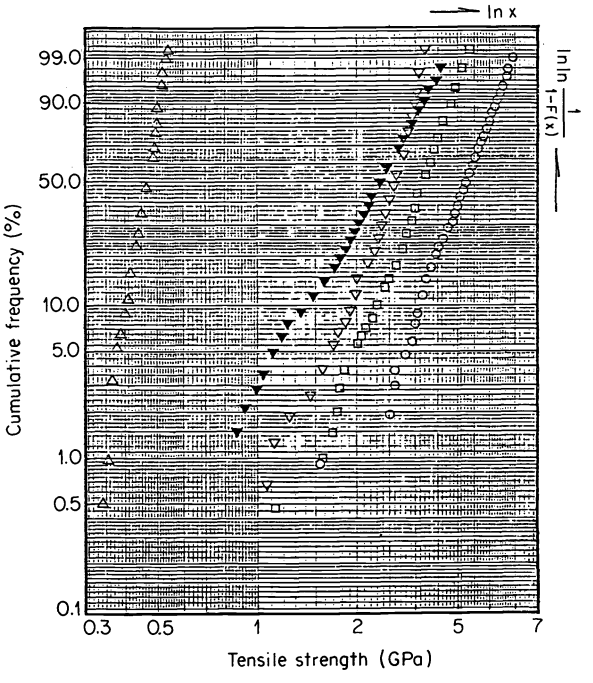

Fig. 33 Tensile strength distribution of carbon fiber single filament

gauge length: 5 cm
○ :A, □ :B, ▼ :C, ▽ :D, △ :E

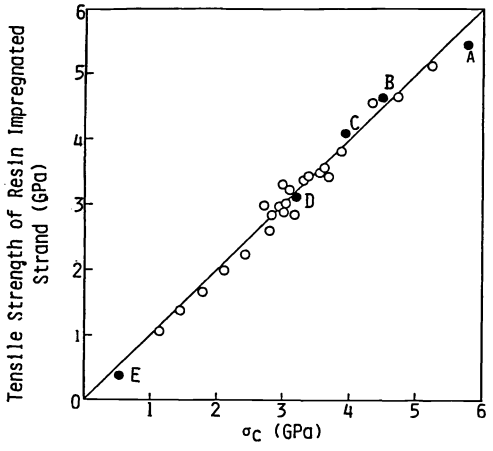

Fig. 34 Relation between measured tensile strength of carbon fiber within composite and calculated value

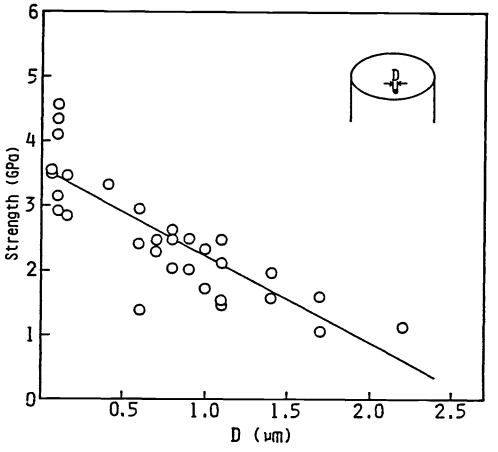

Fig. 35 Dependence of strength on void size

single filaments and then σc were calculated. The calculated bundle strengths σc and observed strand strengths have a good correlation as shown in Fig.34. Samples A, B, C, D and E in Fig.33 and those in Fig.34 correspond each other. Tensile strengths of single filaments of C and D are of the same order but their difference of inclinations of the distribution make tensile strength of resin impregnated strand different.

The Relation of Fiber Tensile Strength to Structural Factors The structural factors which are related to the tensile strength of filaments were discussed by several authors(35-40),but experimental data were not offered enough. In this section experimental analysis about the structural factors of tensile strength of carbon filament yarns are discussed. It is known that macro-defects affect the tensile strength of carbon fibers. In order to make the effect clear, Noguchi et al(41) examined the fracture surface of carbon filaments, and showed that tensile strength decreases as the size of macro-defects which initiate the fracture become large (Fig.35,36).

As shown in these results, the effect of macro-defects is one of the most important factors of tensile strength of carbon fibers. In addition to macro-defects, micro-structure is another important factor. In order to analyze the effect, carbon yarns with different structures and different tensile strength were prepared and their tensile strength and micro-structures were measured(42).

Noguchi et al obtained an experimental equation which shows good correlation between tensile strength and structural parameters of the following form.

$$\sigma_B = 8.4P_{002} - 1300N/C - 0.075I - 235 \qquad (3)$$

The relation between the bundle strength obtained from equation (2) and the calculated strength obtained from equation (3) is shown in Fig.37. Tensile strength

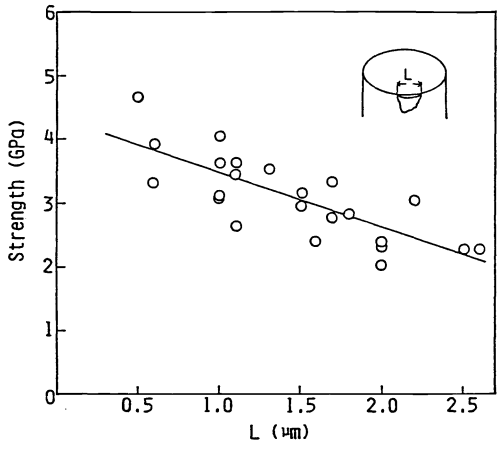

Fig. 36 Dependence of strength on size of extraneous substance

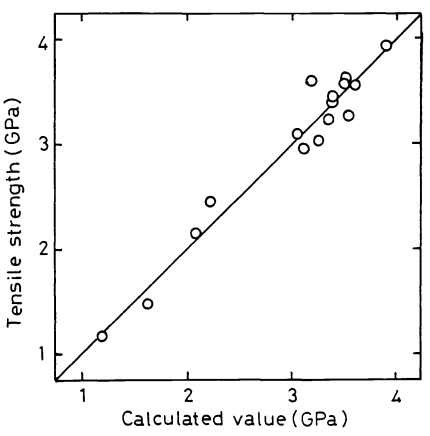

Fig. 37 Relation between tensile strength of carbon fibers (bundle) and calculated value from structural parameters

increases with the decrease of N/C, the weight ratio of nitrogen and carbon, with the decrease of the intensity I of small angle X-ray scattering, and with the increase of the orientation of graphite crystal P_{002}. Coefficient of correlation was 0.96. The good correlation means that these three structural parameters in addition to macro-defects are main factors affecting the tensile strength of carbon filaments.

REFERENCES

1. A. Shindo, Rep. Govn. Ind. Res. Osaka, No. 317 (1961).
2. W. Johnson, L. Phillips and W. Watt, Brit. Pat. 1,110,791 (1964).
3. (a) K. Morita, "Carbon Fibers, the Theory and Application", pp. 47-62, Kindai Henshu Ltd., TOKYO (1984); (b) K. Morita, H. Miyazi and T. Hiramatsu, Carbon, 19, 11 (1981).
4. R. C. Houtz, Textile Res. J., 20, 786 (1950); A. E. Standage and R. Prescott, Nature, 211, 169 (1966); W. Watt, Conf. Industrial Carbon and Graphite (Soc. Chem. Ind., London, 1970); H. N. Friedlander., et. al, Macromol., 1, 79 (1968); A. J. Clark and J. E. Bailey, Nature, 243, 146 (1963); J. W. Johnson et al., Br. Polym. J., 4, 527 (1972); N. Grassie and R. McGuhan, Europ. Polym. J., 3, 1357 (1971).
5. Y. Yokota, I. Shionoya and K. Morita, Extended Abstracts on International Symposium on Carbon, Toyohshi, Japan, Nov. p300 (1982).
6. T. Takagi, I. Shimada, M. Fukuhara, K. Morita and A. Ishitni, ibid., P.321 (1982); to be published in J. Polym. Sci. (1985).
7. A. Ishitani, Carbon 19, 269 (1981).
8. F. Hophgarten, Fibre Science and Technology, 11, 67 (1978).
9. F. Hophgarten, ibid., 12, 283 (1979).
10. K. Waltersson, ibid., 17, 289 (1982).
11. J. M. Thomas, E. M. Evans, M. Barber and P. Swift, Trans Faraday Soc. 67, 1815 (1971).
12. T. Takahagi and A. Ishitani, International Carbon Conference, Bordeaux (1984).
13. F. Tuinstra and J. L. Koenig, J. Chem. Phys., 53, 1126 (1970).
14. M. Nakamizo, R. Kammereck and P. L. Walker, Carbon, 12, 259 (1974).
15. R. F. Nemanich and S. A. Solin, Phys. Rev., B20, 392 (1979).
16. M. Delhaye and P. Dhamelincourt, J. Raman Spectrosc., 3, 33 (1975).
17. G. J. Rosasco, E. S. Etz and W. A. Cassatt, Appl. Spectrosc., 29, 396 (1975).
18. H. Ishida and A. Ishitani, Appl. Spectrosc., 37, 450 (1983); H. Ishida, H. Fukuda, G. Katagiri and A. Ishitani, to be published in Surface Sci., (1985).
19. (a) K. J. Chen and R. J. Diefendorf, "Progress in Science and Engineering of Composits" T. Hayashi, K. Kawata and S. Umekawa, Ed., ICCM-IV, Tokyo, p.97 (1982); (b) B. H. Jones and R. G. Duncan, J. Mat. Sci., 6, 289 (1971).
20. G. Katagiri, H. Ishida and A. Ishitani, Ninth International Conference on Raman Spectroscopy, Tokyo (1984).
21. T. Takahagi and A. Ishitani, Carbon, 22, 43 (1983).
22. A. Proctor and P. M. A. Sherwood, Anal. Chem., 54, 13 (1982).
23. A. Proctor and P. M. A. Sherwood, Surface and Interface Anal., 4, 212 (1982).
24. A. Proctor and P. M. A. Sherwood, Carbon, 21, 53 (1983).
25. D. S. Everhart and C. N. Reilley, Anal. Chem., 53, 665 (1981).
26. K. Murayama et al., Summary of 1st Symposium on Advanced Composites, Japan (1975).
27. L. Drzal, M. J. Rice and P. F. Lloyd, J. Adhesion, 16, 1 (1982).
28. K. Morita, H. Miyachi, K. Kobori, and I. Matsbara, High Temperatures-High Pressures, 9, 193 (1977).
29. P. E. McMahon, A symposium presented at a meeting of commitee D-30 on high modulus fibers and composites SanAntonio, Tex. 1213 April (1972).
30. K, Noguchi, k. Murayama, Summary of 1st Annual conf. of Carbon Soc. Japan (1974).
31. B. W., Rosen, AIAA J., 2, 41 1985 (1964).
32. C. Zweben, B. W. Rosen, J. Mech. Phys. Solids, 18, 189 (1970).
33. S. K. Garg et al, "Analysis of Structural Composite materials" (1973).
34. K. Noguchi, K. Murayama, I. Matsubara, 5th FRP Symposium p. 1. (1976 Osaka Japan).
35. G. A. Cooper, R. M. Meiyer, J. Mater, Sci., 6, 60 (1971).
36. M. Stewart, M. Feughelman, J. Mater, Sci., 8, 1119 (1973).
37. W. N. Reinelds, J. V. Sharp, Carbon, 12, 103 (1974).
38. C. N. Tyson, J. Phys. D., 8, 845 (1975).
39. P. G. Rose, 2nd Intn. Carbon Conf., 294 (1976).
40. F. R., Barnet, M. K. Norr, NOLTR 74-12, AD/A003898.
41. K. Noguchi et al., Carbon 84, Intern. Carbon Conf. , Bordeaux (1984).
42. K. Noguchi, K. Murayama, Summary of Annual Conf. of Sen-i gakkai, P. 300 (June 1978 Japan).